

Spectroscopic and Molecular Characterization of the Oligomeric Antenna of the Diatom *Phaeodactylum tricornutum*[†]

Bernard Lepetit,[‡] Daniela Volke,[§] Milán Szabó,^{||} Ralf Hoffmann,[§] Gyöző Garab,^{||} Christian Wilhelm,[‡] and Reimund Goss^{*‡}

Institute of Biology I, Plant Physiology, University of Leipzig, Johannisallee 21-23, 04103 Leipzig, Germany, Center for Biotechnology and Biomedicine, Institute for Bioanalytical Chemistry, Faculty for Chemistry and Mineralogy, University of Leipzig, Deutscher Platz 5, 04103 Leipzig, Germany, and Institute of Plant Biology, Biological Research Center, Hungarian Academy of Sciences, H-6701 Szeged, P.O. Box 521, Hungary

Received May 3, 2007; Revised Manuscript Received June 15, 2007

ABSTRACT: The photosynthetic antenna system of diatoms contains fucoxanthin chlorophyll *a/c* binding proteins (FCPs), which are membrane intrinsic proteins showing high homology to the light harvesting complexes (LHC) of higher plants. In the present study, we used a mild solubilization of *P. tricornutum* thylakoid membranes in combination with sucrose density gradient centrifugation or gelfiltration and obtained an oligomeric FCP complex (FCPo). The spectroscopic characteristics and pigment stoichiometries of the FCPo complex were comparable to FCP complexes that were isolated after solubilization with higher detergent per chlorophyll ratios. The excitation energy transfer between the FCP-bound pigments was more efficient in the oligomeric FCPo complexes, indicating that these complexes may represent the native form of the diatom antenna system in the thylakoid membrane. Determination of the molecular masses of the two different FCP fractions by gelfiltration revealed that the FCP complexes consisted of trimers, whereas the FCPo complexes were either composed of six monomers or two tightly associated trimers. In contrast to vascular plants, stable functional monomers could not be isolated in *P. tricornutum*. Both types of FCP complexes showed two protein bands in SDS-gels with apparent molecular masses of 18 and 19 kDa, respectively. Sequence analysis by MS/MS revealed that the 19 kDa protein corresponded to the *fcpC* and *fcpD* genes, whereas the 18 kDa band contained the protein of the *fcpE* gene. The presence of an oligomeric antenna in diatoms is in line with the oligomeric organization of antenna complexes in different photoautotrophic groups.

The photosynthetic apparatus of diatoms shares many features with that of green algae and vascular plants, but there are important differences with respect to membrane topology, pigment composition, and organization of the protein-bound pigments. Diatoms possess a chloroplast envelope with four membranes, which results from a secondary endocytobiotic event, where a eukaryotic host cell engulfed a unicellular ancestor of a red alga (1, 2). The diatom thylakoid membranes do not differentiate into stroma and grana thylakoids but are arranged in groups of three (3, 4). Therefore diatoms cannot regulate light harvesting and distribution of the absorbed energy by modulating the ratio of stacked versus unstacked membrane regions as is common in most green algae and vascular plants (5). The pigmentation of diatoms differs in two important aspects from that of vascular plants: they do not possess Chl *b*¹ but use Chl *c* as accessory pigment, and their antenna systems contain high amounts of xanthophylls, with fucoxanthin being the main

light harvesting pigment (hence the name fucoxanthin Chl *a/c* binding protein complexes, FCP complexes).

Analyses of the *fcp* genes showed that more genes exist than the two or three apoproteins, which are usually detected in diatom thylakoid membranes by conventional biochemical methods (6–9). Although the amino acid sequences of the FCPs and LHC proteins show significant homologies, the resulting mature FCPs have smaller apparent molecular masses of 17–22 kDa compared to the LHC proteins of vascular plants (24–29 kDa). For *P. tricornutum*, two or three FCPs with molecular masses between 17.5 and 19.5 kDa have been described (10–12).

Like the LHC proteins of vascular plants, the FCPs are integrated into the thylakoid membrane by three membrane spanning α -helices. Because of the existence of significant sequence similarities between FCPs and LHC proteins, which are especially pronounced in the regions of helix 1 and 3,

[†] This work was supported by a grant from the Hungarian Fund for Basic Research OTKA K63252 and MÖB-DAAD 9/2006. The Marie Curie grant MCRTN-CT-2003-505069 is also gratefully acknowledged.

* Corresponding author. Tel: +49 341 9736873. Fax: +49 341 9736899. E-mail: rgoss@rz.uni-leipzig.de.

[‡] Institute of Biology I, University of Leipzig.

[§] Center for Biotechnology and Biomedicine, University of Leipzig.

^{||} Hungarian Academy of Sciences.

¹ Abbreviations: β -Car, β -carotene; Chl *a*, chlorophyll *a*; Chl *c*, chlorophyll *c*; DDE, diadinoxanthin de-epoxidase; Ddx, diadinoxanthin; Dtx, diatoxanthin; DM, *n*-dodecyl β -D-maltoside; FCP, fucoxanthin chlorophyll *a/c* binding protein; Fd, Ferredoxin; FP, free pigment; Fx, fucoxanthin; HL, high light; LHC, light harvesting complex; LL, low light; NPQ, non-photochemical chlorophyll fluorescence quenching; PAR, photosynthetically active radiation; PS, photosystem; SDC, sucrose density gradient centrifugation; VDE, violaxanthin de-epoxidase; Vx, violaxanthin; XC, xanthophyll cycle.

the FCPs can be regarded as members of the LHC protein superfamily (13, 14). In vascular plants, both PSII and PSI are organized into large supercomplexes with variable amounts of their own peripheral antenna complexes, LHCII and LHCI, respectively. The PSI supercomplex is located in the unstacked (stroma) region and contains a core complex that binds single copies of four different LHCI proteins (15). PSII supercomplexes are predominantly located in the stacked (granum) region and consist of the dimeric PSII core complex, minor, monomeric LHCII proteins, CP 26 and CP 29, and two to four copies of the major trimeric LHCIIb (15). The LHCII-PSII supercomplexes often associate into megacomplexes and semicrystalline domains. The additional LHCIIb trimers, that is, those that are not bound to the supercomplexes but are located in the stacked region, also form large ordered arrays, LHCII-only macrodomains (16, 17). Presently, there is no evidence for a PSII or PSI specific antenna in diatoms, but recently, some progress has been made with respect to the (macro-)organization of the FCP complexes in the native thylakoid membrane. Büchel (2003) reported on oligomeric and trimeric FCP complexes in *C. meneghiniana* that were separated by sucrose gradient centrifugation (18). By direct gel filtration, Guglielmi et al. (2005) isolated a trimeric FCP complex from *P. tricornutum* (19). They also found some indications for the existence of minor antenna proteins in diatoms, which could be comparable to the minor LHCII proteins of vascular plants.

In addition to their role in light harvesting, the FCP complexes are also the sites of photoprotection under excess light, converting absorbed quanta into heat. The most important photoprotection mechanism of diatoms is the Ddx cycle, in which the epoxidized Ddx is converted to the de-epoxidized Dtx during HL illumination (20). De-epoxidation of Ddx to Dtx is directly correlated with NPQ, the non-photochemical quenching of Chl fluorescence, which leads to a harmless thermal dissipation of light energy absorbed in excess (21, 22). Similar to vascular plants, the xanthophyll cycle (XC) pigments are assumed to be localized in the antenna complexes (23).

In vascular plants, the minor LHCII proteins, which connect the peripheral antenna to the PSII core complex (15), are enriched in the Vx cycle pigments. The peripheral antenna complexes, however, show a higher de-epoxidation state of the XC pigment pool after HL illumination, indicating that they represent the main site of XC-mediated photoprotection (24).

It was the aim of the present work to collect further data on the native state of diatom antenna complexes with special focus on the possible existence of oligomeric FCP complexes. To achieve this, low concentrations of the mild detergent *n*-dodecyl β -D-maltoside (DM) were used to solubilize isolated thylakoid membranes of *P. tricornutum*, followed by sucrose gradient centrifugation or direct gelfiltration. Another focus of the present study was to determine the protein composition of the complexes and to assign them to their respective genes by direct protein sequencing using MS/MS, to our knowledge, for the first time in diatoms. Finally, the different purified pigment–protein complexes were analyzed with respect to their pigment composition to answer the question where the Ddx cycle pigments are located and how they are converted under high light conditions by the de-epoxidation reaction.

MATERIALS AND METHODS

Plant Material. *Phaeodactylum tricornutum* cells (1090-1a), obtained from Culture Collection of Algae, Göttingen (SAG, FRG) were grown in ASP-Medium according to Provasoli et al. (25) with the modifications introduced by Lohr and Wilhelm (26). Cells were cultivated as batch cultures at a light intensity of $40 \mu\text{mol m}^{-2} \text{s}^{-1}$ photon flux density of the photosynthetically active radiation (PAR) in a light/dark regime of 14/10 h. The temperature of the growth chamber was adjusted to 20 °C.

Preparation of Pigment–Protein Complexes. Isolation of thylakoid membranes from *P. tricornutum* was performed according to Büchel (18) with some modifications. Cells from the logarithmic growth phase (45 min low-light adapted, except in illumination experiments) with a Chl concentration of 4–5 mg L⁻¹ were harvested by centrifugation (4000g, 5 min). All following preparation steps were carried out in dim light and at 4 °C. The cells were resuspended in isolation medium A (10 mM MES at pH 6.5, 2 mM KCl, 5 mM EDTA, and 1 M Sorbitol) and disrupted in a French pressure cell at 12,500 psi. Unbroken cells were separated from broken cells by a centrifugation step at 1000g for 10 min, then resuspended in isolation medium A, and passed through the French press for a second time. After centrifugation, the supernatants of both centrifugation steps were merged and centrifuged at 40,000g for 20 min. Finally, the pelleted thylakoids were resuspended in a small amount of isolation medium B (10 mM MES at pH 6.5, 2 mM KCl, and 5 mM EDTA), and Chl concentration was determined.

For the solubilization of thylakoid membranes, equal amounts of isolated thylakoids, corresponding to 0.5–1 mg of total Chl, were centrifuged for 20 min at 40,000g. The pelleted thylakoids were resuspended in *n*-dodecyl β -D-maltoside (DM) to yield the final detergent/Chl ratios of 5, 10, 20, and 40, corresponding to 0.5, 1, 2, and 4% DM (w/v), respectively. The thylakoids were solubilized on ice for 20 min under continuous stirring. After solubilization, the membranes were centrifuged at 40,000g for 20 min. The supernatant, containing the solubilized pigment–protein complexes, was collected and immediately applied to the sucrose gradients used for sucrose density gradient centrifugation (SDC).

In the present study, a linear sucrose gradient from 0 to 0.7 M sucrose (w/v, in isolation medium B, complemented with 0.03% DM) was used. The samples were centrifuged for 19 h at 110,000g using a swing-out rotor. After the separation, sucrose gradient bands were harvested with a syringe and immediately characterized by UV–vis absorbance and fluorescence spectroscopy. To confirm the results obtained by SDC, thylakoids corresponding to a Chl content of 250 μg were solubilized with a DM/Chl ratio of 5, 10, 20, and 40, corresponding to 0.5, 1, 2, and 4% DM (w/v), respectively, and loaded on a Superdex 200 HR 10/30 column (Amersham) attached to an FPLC system (Biorad). Gelfiltration was performed in isolation medium B of the thylakoid preparation supplemented with 0.03% DM at a flowrate of 0.2 mL min⁻¹. The temperature was carefully adjusted to 4 °C. Calibration of the column was achieved by using the Sigma gelfiltration molecular weight markers (MW-GF-1000). The sample containing the calibration proteins was supplemented with 2% DM. This corresponds

to the DM concentration of thylakoid samples, which were solubilized with a DM/Chl ratio of 20. For additional calibration and comparison, gelfiltration was also carried out with solubilized spinach thylakoids (DM/Chl ratios of 20 and 40, respectively), which were isolated according to Jensen and Bassham (27).

Spectral Characterization of Pigment–Protein Complexes. Chlorophyll determination was carried out according to Jeffrey and Humphrey (28). Absorption spectra were recorded with a Specord M 500 spectrophotometer (Zeiss, FRG) in a wavelength range from 350 to 750 nm. The bandwidth was set to 1 nm.

Low-temperature fluorescence spectra were recorded with an F-3000 fluorescence spectrophotometer (Hitachi, Japan) at 77 K after diluting the sample in glycerine to achieve a final glycerine concentration of 60% (v/v) and a Chl concentration of $1 \mu\text{g mL}^{-1}$. Fluorescence emission spectra were recorded in the wavelength range from 600 to 800 nm with an excitation wavelength of 440 nm and an excitation and emission bandwidth of 10 and 3 nm, respectively. For the sampling of fluorescence excitation spectra, the constant emission wavelength was set to the Chl *a* fluorescence emission maximum. Excitation spectra were recorded in the wavelength range from 360 to 560 nm with settings of the excitation and emission bandwidths of 3 and 10 nm, respectively. The excitation spectra were corrected using a rhodamine B spectrum as a reference.

CD spectra were measured at room temperature in a CD6 dichrograph (Jobin-Yvon) in the wavelength range from 400 to 750 nm with a bandwidth setting of 2 nm. The Chl content of the fractions was adjusted to $20 \mu\text{g mL}^{-1}$.

Pigment Analysis. Pigments were extracted by addition of 500 μL ethylacetate, 500 μL distilled water, and a spatula tip of NaCl to 250 μL of the different fractions collected from the sucrose gradients. The samples were stirred several times to transfer the pigments into the organic phase and afterward centrifuged for 2 min at 20,000g. The organic phases were collected and the pigments dried in a gentle N_2 stream and stored at -80°C until HPLC analysis. The dried pigments were dissolved in HPLC-extraction medium [90% methanol/0.2 M ammoniumacetate (90/10, v/v) and 10% ethylacetate] and analyzed on a Waters 600 MS chromatography system equipped with a Waters 996 photodiode array detector (Waters Millipore, FRG) and an ET 250/4 Nucleosil 300-5 C_{18} column (Macherey-Nagel, FRG). Eluents and gradient programs were as described in Kraay et al. (29), and pigments were quantified according to Lohr and Wilhelm (26) and Wilhelm et al. (30).

To analyze the de-epoxidation state (DES) of the Ddx cycle pigment pool of different pigment–protein complexes, cells were illuminated with a light intensity of $1000 \mu\text{mol m}^{-2} \text{s}^{-1}$ PAR for 30 min. After the end of the HL period, thylakoids were immediately prepared according to the procedure described above. After the separation of the pigment–protein complexes, pigments were extracted and analyzed by HPLC.

Gel Electrophoresis. The protein composition of the isolated photosynthetic pigment–protein complexes was determined by SDS–PAGE following the method of Laemmli (31), using a 15% separating gel and a 4% stacking gel. The separated proteins were stained with Coomassie using the ImperialTM protein stain kit (Pierce).

Mass Spectrometry. Protein bands of interest were excised from the SDS gels of the SDC fractions and analyzed by MALDI-TOF/TOF–MS (4700 Proteomics Analyzer, Applied Biosystems, FRG). Briefly, 100 μL of ammonium bicarbonate buffer (pH 7.5, 50 mM) containing 30% acetonitrile was added to each tube and incubated at 37°C for 15 min. The solution was discarded and the step repeated until the spots were completely destained. Then, 100 μL of acetonitrile were added to each sample, incubated at room temperature for 15 min, the supernatant was discarded, and the spots were dried in a Speedvac. Trypsin (100 to 200 ng) (Promega, FRG) dissolved in 3 mM ammonium bicarbonate buffer (pH 7.5) was added. After 5 min of rehydration, the sample was diluted with 10–20 μL of ammonium bicarbonate buffer (3 mM, pH 7.5), and the proteins were digested for 4 h at 37°C . The digest was stopped by adding 20 μL of 50% aqueous acetonitrile containing 0.3% trifluoroacetic acid (TFA) and incubated at 37°C for 15 min. The supernatant was lyophilized and dissolved directly in 2 μL of matrix solution (α -cyano-4-hydroxy cinnamic acid, CHCA, Bruker Daltonics, FRG, 4 mg mL^{-1} in 50% acetonitrile containing 0.1% TFA), spotted on a stainless steel MALDI target, and air-dried at room temperature.

The mass analysis was performed in reflector mode at an accelerating voltage of 20 kV, 70% grid voltage, and a delay time of 1.277 ns on the MALDI-TOF/TOF–MS. MS spectra were generated by accumulating 2000 laser shots and MS/MS spectra with 3000 laser shots. MS and MS/MS data were analyzed by the Data Explorer Software, version 4.6 (Applied Biosystems, USA) and the MASCOT database search engine (Matrix Science, UK) against the Swiss-Prot or MSDB database with the following search parameters: maximum of two missed trypsin cleavage and possible methionine oxidation. The peptide tolerance was set at ± 100 ppm and MS/MS tolerance at ± 0.25 Da.

RESULTS

The detergent *n*-dodecyl β -D-maltoside (DM) was used in different concentrations to solubilize the pigment–protein complexes of thylakoid membranes of *P. tricornutum*. Using a linear sucrose gradient from 0 to 0.7 M sucrose, typically three to four different fractions could be separated depending on the solubilization conditions (Figure 1). The solubilization conditions used in the present study yielded low amounts of free pigment (FP), which were found as a small yellow-green fraction on top of the sucrose gradient. When a detergent/Chl ratio of 20 was used, the gradient was dominated by a broad dark brown band, which was located underneath the FP fraction and contained roughly 80% of the total Chl *a* (Figure 1A). This fraction, on the basis of its typical spectroscopic features of diatom antenna proteins, was designated as the FCP fraction. At higher densities in the sucrose gradient, we typically observed two green bands, the upper band representing PSII core complexes, while the lower band was enriched in PSI. However, a clear separation of the photosystems could not be achieved. Thus, for further pigment and protein analysis, the fraction enriched in PSI was used (to avoid contamination with the FCP fraction) and termed the PS fraction.

A significantly different band pattern was found when the thylakoids were solubilized under milder conditions, with a

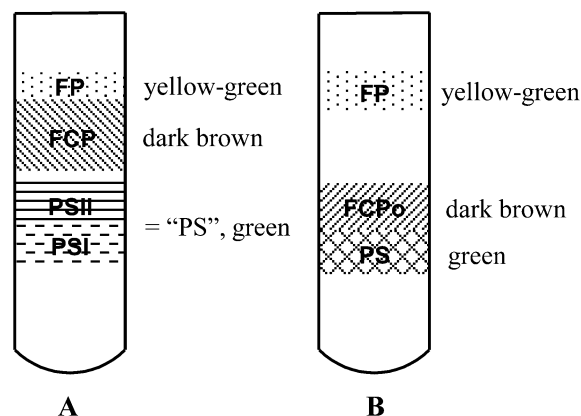


FIGURE 1: Schematic representation of the different fractions obtained by sucrose density gradient centrifugation (linear gradient from 0 to 0.7 M sucrose) of *P. tricornutum* thylakoids, which were solubilized with a DM/Chl ratio of 20 (A) and 5 (B). The abbreviations used for the fractions are FP, free pigment; FCP, fucocanthin chlorophyll binding protein complex; FCPo, oligomeric FCP; and PS (I,II), photosystem (I,II).

detergent/Chl ratio of 5 (Figure 1B). After separation of the proteins, the dark brown fraction was found in the lower part of the sucrose gradient. It was visible as a discrete band in the region of the PSII core complex and was designated as FCPo (for the oligomeric FCP complex) because of its high density in the sucrose gradient, which indicates a high molecular mass of the complex. With this mild solubilization, only one PS fraction was observed, which consisted mainly of PSI, as indicated by a pronounced shoulder at 710 nm in the low-temperature fluorescence emission spectrum (data not shown). This fraction was found at slightly higher densities in the gradient, possibly due to an enrichment in pigments, lipids, and proteins compared to that in the PS fraction obtained at higher detergent concentrations. We also tested DM/Chl ratios of 10 and 40, respectively (data not shown). The solubilization with a DM/Chl ratio of 40 yielded a fractionation pattern similar to that of the solubilization with a ratio of 20. Decreasing this ratio to 10 resulted in the appearance of a broad brown-colored fraction located between the FP band and the PSII fraction.

To gain further insight into the degree of oligomerization of the two FCP preparations, gel filtration was performed (Figure 2) with thylakoids, which were solubilized with the same DM/Chl ratios as those in the SDC. The elution profile of the separated pigment–protein complexes was virtually identical when DM/Chl ratios of 20 or 40 (not shown) were used. First, two small peaks (designated 1 and 2 in Figure 2) eluted from the column. Both of these fractions were green and contained the PSI and II core complexes (fractions 1 and 2, respectively), as judged by their absorption and low-temperature fluorescence spectra (data not shown). The two green fractions were followed by a highly concentrated fraction (fraction 5) with a brown color that contained FCP complexes. When the DM/Chl ratio was decreased to 5, the elution time for the photosystems remained virtually unchanged, while the FCP fraction eluted significantly earlier (fraction 3). This clearly shows that the FCPo complex (fraction 3) possessed a higher molecular mass than the FCP complex (fraction 5). The FCPo eluted at a buffer volume comparable to that of the PSII core complex isolated after solubilization with a DM/Chl ratio of 20. This indicated that

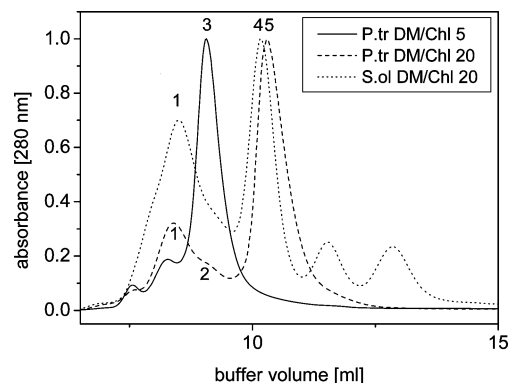


FIGURE 2: Gelfiltration elution profile of *P. tricornutum* (P.tr) thylakoids solubilized with a DM/Chl ratio of 5 and 20, respectively, and *Spinacia oleracea* (S.ol) thylakoids solubilized with a DM/Chl ratio of 20. The numbers depicted denote different pigment–protein complex fractions: 1, PSI; 2, PSII; 3, FCPo complex; 4, LHCIIB trimer; and 5, FCP complex.

the molecular masses of the FCPo and the PSII cores were comparable. Using a calibration curve with standard proteins of known molecular masses, we were able to calculate the masses of the separated pigment–protein complexes. This calculation yielded molecular masses of approximately 620 and 440 kDa for PSI and PSII, respectively. The FCPo complex had a similar mass as PSII, whereas for the FCP complex from fraction 5, a mass of only 230 kDa was calculated, indicating a significantly lower degree of oligomerization in this fraction. It is important to note that, regardless of the solubilization conditions, only one discrete FCP fraction occurred, which can be considered as a peripheral antenna, that is, neither a mixture of the two oligomeric states nor monomeric FCP complexes were observed. In order to obtain further information about the size of the FCP complexes, spinach thylakoids were isolated and solubilized with DM/Chl ratios of 20 and 40, respectively. In both cases, PSI and PSII eluted approximately at the same time compared to that in *P. tricornutum*, while the trimeric LHCIIB (fraction 4 in Figure 2) eluted just slightly earlier than the FCP fraction with lower degree of oligomerization. During the separation of spinach proteins, two additional pigment–protein fractions were observed, which eluted after the LHCIIB trimers. These two fractions most probably represent dimeric and monomeric LHCI and II proteins, respectively. According to the present calibration curve, the solubilized LHCIIB trimer in the detergent micelle had a molecular mass of 245 kDa. Taking together the information of the different gelfiltrations, we conclude that the organizational state of the FCP complex in fraction 5 is trimeric, whereas the FCPo complex consists of either a hexamer or two closely associated trimers.

As shown in Figure 3A, the FCPo and FCP fractions exhibited comparable absorption spectra. Both spectra were dominated by Chl *a* absorption, which showed maxima around 440 and 672 nm in the blue and red parts of the spectrum, respectively. The existence of high xanthophyll and Chl *c* concentrations bound to the FCP complexes became visible as pronounced shoulders at 465 (Chl *c*) and 490 nm (xanthophylls). Whereas the shoulder at 490 nm could be attributed to shorter wavelength-absorbing xanthophylls like Ddx, the absorption at wavelengths above 500 nm was exclusively due to high concentrations of the long

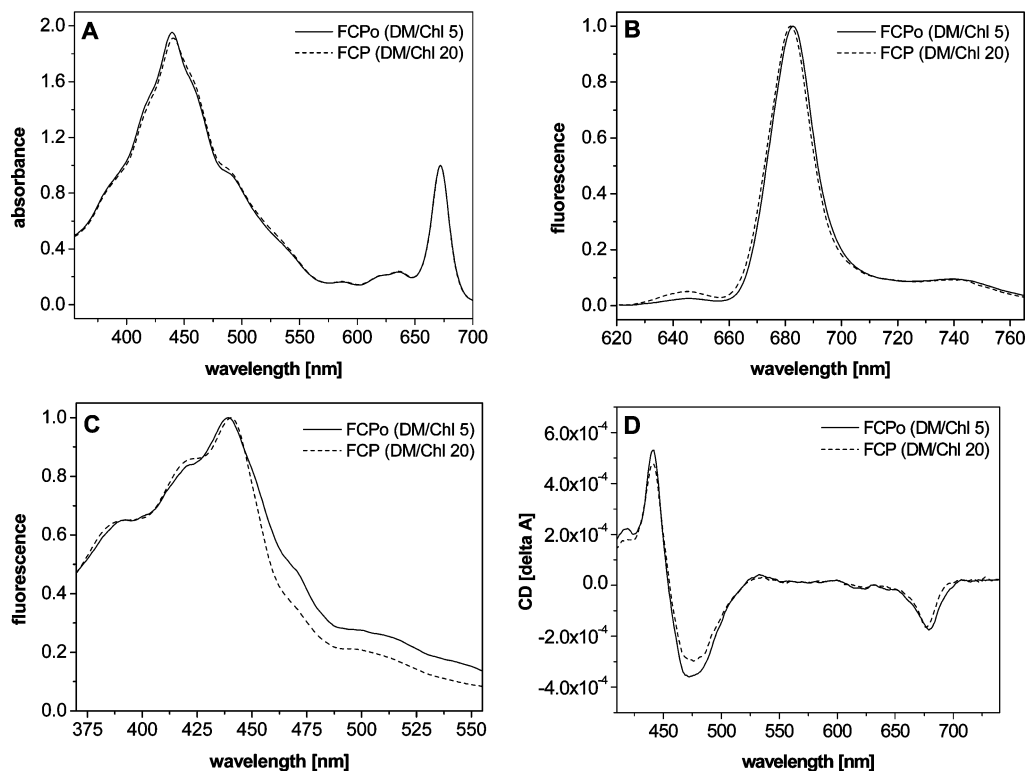


FIGURE 3: Comparison of the FCP and FCPo fraction obtained after SDC (see Figure 1) with different spectroscopic means. For details, see Materials and Methods. (A) Absorption spectra normalized to the Chl *a* maximum in the red part of the absorption spectrum. (B) Fluorescence emission spectra (77 K). The excitation wavelength was 440 nm and the spectra were normalized to the respective fluorescence emission maximum. (C) Fluorescence excitation spectra (77 K). The fluorescence emission wavelength was set to 682 nm for both the FCPo and FCP complexes. The spectra were normalized to their respective maxima in the blue part of the spectra. (D) CD spectra. The Chl content of the two fractions was adjusted to the same value, 20 $\mu\text{g mL}^{-1}$.

wavelength-absorbing Fx. Small differences between the two FCP fractions were found in the blue part of the spectrum where FCPo exhibited lower absorption in the wavelength range between 450 and 550 nm. These were due to a comigration of the FCPo with the PSII, which resulted in an apparently higher Chl *a* content (see also Figure 4).

The low-temperature fluorescence emission spectra of the two FCP fractions were also very similar to each other (Figure 3B), both showing a single Chl *a* fluorescence emission maximum at 682 nm. However, the FCP complex obtained after solubilization with a DM/Chl ratio of 20 exhibited a low but clearly visible Chl *c* fluorescence emission at 645 nm. This indicates that the harsher solubilization conditions perturbed the excitation energy transfer of part of the Chl *c* molecules to Chl *a*, most probably caused by an alteration of their binding to the protein. In contrast, the FCPo complexes exhibited almost no Chl *c* fluorescence emission, showing that Chl *c* remained in its functional state.

Low-temperature fluorescence excitation spectra revealed small but significant alterations in the binding of accessory pigments of the FCPo compared to the trimeric FCP. They show that the energy transfer from Fx and Chl *c* to Chl *a* was significantly better in the FCPo complexes (Figure 3C), which was indicated by the more pronounced shoulders between 460 and 550 nm. It is interesting to note that the shoulder at around 490 nm, which was clearly visible in the absorption spectra (Figure 3A), could not be detected in the excitation spectra of either FCP fractions, indicating that the majority of Ddx molecules that were responsible for this absorption do not transfer their excitation energy to Chl *a*.

The CD spectra of the FCPo and FCP were also very similar to each other (Figure 3D) and to the FCP of *C. menhianiana* (18). Minor differences between FCPo and FCP fractions could be observed both in the red and the Soret regions. In the red region, they could be accounted for by a contamination of the FCPo fraction with the reaction center complexes. On the basis of an inspection of the difference spectra (not shown) between FCPo and FCP, it was estimated that FCPo on a Chl basis contained about 5–8% core complexes, which is in good accordance with the finding that FCPo partially co-purifies with the PS fraction (Figures 1 and 2). In contrast, the differences in the Soret region could not be assigned to this overlap but appeared to originate from small alterations in the excitation interactions. This notion is supported by the observation that isolated thylakoid membranes upon varying the ionic strength of the medium exhibit well discernible spectral variations in the same region (data not shown). Nevertheless, the presently available data do not allow us to establish a spectral fingerprint of the higher oligomeric state of FCP, and thus, we conclude that the excitonic interactions in FCPo and FCP are very similar to each other.

To obtain further information about the pigment composition of the two different FCP preparations, the pigment stoichiometries were determined by HPLC analysis (Figure 4). The pigment composition of the FCPo and the FCP fractions was found to be almost identical. Both, the oligomeric and the trimeric FCP complexes contained Fx in slightly higher concentrations than Chl *a*. They bound around 300–350 mmol Chl *c* per mol Chl *a* and 160–200 mmol XC pigments (Ddx+Dtx). The ratio of Fx to total XC

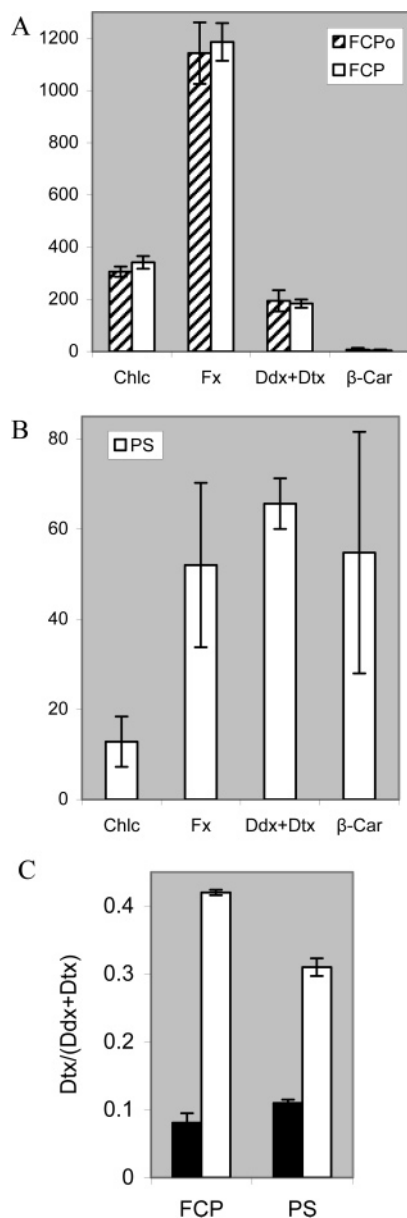


FIGURE 4: Pigment composition of the FCP, FCPo, and PS fractions obtained after solubilization and SDC, and the de-epoxidation state of the Ddx cycle pigment pool (DES). Pigment values are depicted in mmol pigment per mol Chl α , the mean values were obtained from three independent pigment–protein complex preparations. (A) Comparison of the FCPo complexes isolated from thylakoids solubilized with a DM/Chl ratio of 5 with the FCP complexes (DM/Chl ratio 20). (B) Pigment composition of the PS fractions obtained after solubilization with a DM/Chl ratio of 20. (C) DES of PS and FCP fractions (white bars) obtained after 30 min of HL illumination with $1000 \mu\text{mol m}^{-2} \text{s}^{-1}$ PAR. As a control, the dark adapted fractions (black bars) are depicted.

pigments was found to be between 6 and 7 for both the FCPo and the FCP fractions; the amount of β -Car bound to the antenna proteins was negligible. Small differences in the pigment composition can be explained by the partial comigration of the core complexes and the FCPo (see above).

To characterize the proteins that build up the antenna and the photosynthetic core complexes, SDS–PAGE followed by MS/MS was carried out. The polypeptide composition of the FCPo and FCP complex was virtually identical: only very low amounts of the comigrating photosystem proteins could be seen in the FCPo fraction (Figure 5B). The FCP

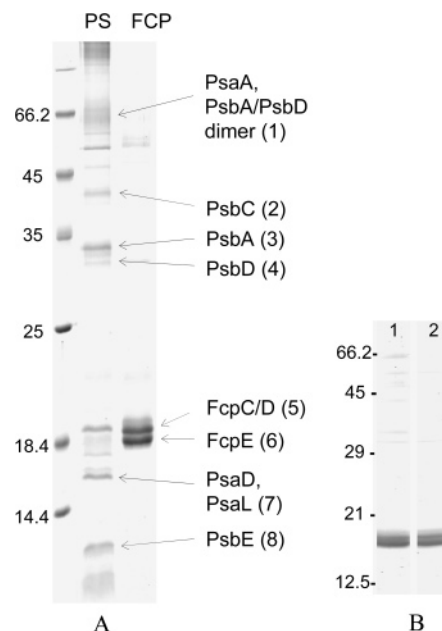


FIGURE 5: SDS–PAGE of the PSI and FCP fractions obtained by SDC after thylakoid solubilization with a DM/Chl ratio of 20 (A) and of the FCPo and FCP fractions (B). Gels were stained with Coomassie blue. Samples with comparable Chl concentrations ($4\text{--}5 \mu\text{g}$) were applied to the gels. (A) Protein pattern of the fractions. Bands that were assigned by MS/MS are indicated. Molecular weight markers are shown in the left lane of the gel (in kDa). Note that the polypeptide pattern of the PSI fraction is comparable to that of the PS fraction derived from a solubilization with a DM/Chl ratio of 5 (see Figure 1). (B) Polypeptide pattern of the FCPo (1) and FCP (2) complexes, respectively. Molecular weight markers are indicated on the left side of the gel, and the numbers on the top of the gel correspond to the respective FCP fractions: 1, FCPo (DM/Chl 5) and 2, FCP (DM/Chl 20).

fractions contained two different apoproteins with molecular masses in the 20 kDa range. According to the terminology of Fawley and Grossman (11), these apoproteins represent the 19 and 18 kDa FCP polypeptide, respectively. A third, much weaker band appeared slightly above the 19 kDa FCP. The lack of additional protein bands in the FCP and FCPo fractions indicated that the peripheral antenna complexes were exclusively composed of proteins with masses around 18–19 kDa. The identity of the FCP bands was confirmed by sequence analysis with mass spectrometry. The mass spectra of the digested 19 kDa FCP band displayed several signals for the gene products of the *fcpC* and *fcpD* genes, which were further confirmed by tandem mass spectrometry, selecting the most intense signals (Table 1). However, some weak signals not matching either of these two proteins also indicated the presence of *fcpB* and *fcpE* gene products. The digest of the 18 kDa FCP band contained mostly the product of the *fcpE* gene, but also some minor signals specific for the *fcpA* and *fcpF* genes.

The SDS–PAGE of the PS fraction (Figure 5A) confirmed that SDC did not completely separate the two photosystems. The PS fraction depicted in Figure 5A was mainly composed of PSI, according to its location in the gradient and its spectroscopic characteristics, but also contained proteins belonging to PSII. This was confirmed by mass spectrometry, where it was possible to identify D1, D2, CP43, and cytochrome b559 as PSII proteins, while for PSI PsaA, PsaD and PsaL were detected (Table 1). Only trace amounts of proteins in the range of 18 to 19 kDa were visible. However,

Table 1: Assignment of the Protein Bands of the SDS-PAGE to the Respective Genes^a

gelband no.	protein identification no.	protein	sequence	peptide-mass
1	A0T0L9_PHATR	PsaA (PSI P700 A1 protein)	LLDAGVAPQEIPLPHEFLINR	2342.38
	A0T0G9_PHATR	PsbA	VINTWADIINR	1314.80
	A0T097_PHATR	PsbD	AWMAAQDQPHENFVFPEEVLP	2611.44
2	A0T096_PHATR	PsbC (CP43)	IKNDIQPWQER	1426.71
			DIESTGFAWWSGNAR	1696.75
			SPSGEIIFGGETMR	1480.68
3	A0T0G9_PHATR	PsbA (PSII D1 protein)	FGQEEETYNIIVAAHGYFGR	2188.17
			LIFQYASFNNR	1459.87
			ETTENESTNYGYK	1547.82
4	A0T097_PHATR	PsbD (PSII D2 protein)	AAEDPEFETFYTK	1547.68
			NILLNEGIR	1041.62
			AWMAAQDQPHENFVFPEEVLP	2611.23
5	Q08586/Q08587_PHATR ^b	FcpC/D	ISMLAVVGYLVEAGVR	1821.03
			NGAIDFGWDTFDEETQFK	2120.05
			DLTGAEFVGDFR	1455.71
6	Q41093_PHATR ^b	FcpE	NDFIDFGWDSFDEETK	1964.93
7	A0T0B9_PHATR	PsaD (PSI Fd-binding protein)	IFPSGEVQYLHPK	1514.78
	A0T0M6_PHATR	PsaL ^c	FGLTPLLR	916.13
	P49486_ODOSI		AILKNLPAYR	1158.65
8	A0T0A3_PHATR	PsbE (cytochrome b559 alpha chain)	QQIPLVNDR	1082.58
			PNEYFTQDR	1169.51

^a The sequences were obtained by means of MALDI-TOF/TOF-MS. The protein identification number is obtained from the Swiss-Prot database. Peptide-mass is indicated in Da. ^b The peptide masses of nuclear encoded proteins refer to the respective precursor proteins, not the mature oroteins. ^c Function is still under debate.

the PS fractions contained a 19–19.5 kDa protein, which occurred in significant concentrations. Several attempts were made to identify the nature of this protein by MS/MS, but the mass fragments obtained were not suitable to generate amino acid sequences of sufficient quality.

With respect to the xanthophyll composition, significant differences could be observed between the peripheral antenna and the PS core complexes (Figure 4). The PS fractions showed higher Ddx and Dtx concentrations when calculated on a Chl *c* and Fx basis. The Fx per Ddx + Dtx ratio was around 1 in the PS fraction (Figure 4B), whereas the FCP and FCPo bands exhibited ratios of 6–7 to 1 (Figure 4A). This means that the PS fractions contained equal amounts of XC pigments and Fx, whereas the FCP fractions contained significantly more Fx than Ddx + Dtx. However, because of the much higher concentration of proteins of the peripheral antenna, the majority of XC pigments are bound to the FCPo or FCP. In order to examine if HL illumination affects the oligomeric state of the FCPs, thylakoids were prepared from dark adapted and illuminated cells, respectively. HL illumination had no effect on the fractionation pattern in the sucrose gradient. However, by comparing the pigment composition of these protein fractions, it became obvious that the FCP and FCPo complexes exhibited an approximately 35% higher de-epoxidation state of the Ddx cycle pigment pool (DES) compared with that of the PS fractions (Figure 4C). From the HPLC data, we conclude that a protein, which is enriched in the XC pigments but exhibits a low DES, is tightly bound to the PS core complexes. One likely candidate for such a protein is the 19.5 kDa protein, which appears in the PS fractions (Figure 5A). However, this protein band could not be unequivocally assigned by MS/MS (see above) so that the nature of the Ddx binding protein remains to be clarified.

DISCUSSION

In the present article, we report on the isolation of an oligomeric FCP complex (FCPo) from the diatom *P. tricornutum*, which was obtained after solubilizing thylakoid membranes with a mild detergent treatment, and a trimeric antenna complex obtained after harsher solubilization. Oligomeric FCP complexes from two different diatoms have recently been isolated. Büchel (18) presented evidence for the existence of oligomeric FCP complexes in *C. meneghiniana* after solubilizing thylakoids with a DM/Chl ratio of 40. These oligomeric complexes consisted of tightly assembled FCP trimers, which, nevertheless, exhibited a significantly lower molecular mass in a sucrose gradient than the two PS fractions. Guglielmi et al. (19) reported on the existence of small oligomeric antenna complexes in *P. tricornutum*. Although these authors also used DM/Chl ratios, which in the present experiments prevented the purification of FCPo complexes, oligomerization was induced by exposing the FCPs to high salt concentrations or a combination of high salt concentration and short solubilization time. Salt-induced oligomeric FCP complexes were then prepared by SDC or gelfiltration and had apparent sizes in the range of dimeric or trimeric LHCII complexes, respectively (19).

The FCPo complex of this work, isolated by mild detergent treatment with a DM/Chl ratio of 5, shows a considerably higher degree of oligomerization than the oligomeric complexes isolated by Büchel (18) and Guglielmi et al. (19) when the localization of the complexes in a sucrose gradient is compared. An oligomeric antenna with a molecular mass similar to that of the native PSII core complex was not described so far, neither for *P. tricornutum* nor for *C. meneghiniana*. However, when a comparison of the gelfiltration data of the present study with that in the literature is performed, the oligomeric and trimeric FCP fractions strongly resemble the complexes found in *C. meneghiniana*. In *C.*

meneghiniana, trimeric FCP fractions were found as well as oligomeric complexes composed of six to nine FCPs (18). The trimeric FCP complex of *P. tricornutum* isolated in the present work has a molecular mass of 230 kDa, which is around 15 kDa less than the mass of the LHCIIb trimer isolated as a control pigment–protein complex. The latter value is in accordance with data obtained for the LHCIIb trimer by blue native PAGE, which suggests a molecular mass of 280 kDa for the trimeric complex (32). (Note that in this study, the molecular masses of PSI (700 kDa) and PSII (480 kDa) are also slightly higher than our data from gelfiltration.) Taking into account that the solubilized complexes consist of proteins, pigments, unknown concentrations of lipids, structural water, and detergent, the values of the present study are within the limits of experimental variations. The slightly lower mass of the trimeric FCP complex compared to that of the LHCIIb trimer is most probably due to the lower mass of the respective apoproteins. The FCPo complex of *P. tricornutum* has a molecular mass of approximately 440 kDa. This shows that the FCPo is most likely composed of six FCPs, which again resembles the situation in *C. meneghiniana*. However, using a DM/Chl ratio as described in ref 18 for *P. tricornutum*, we could never obtain higher oligomeric complexes but only observed FCP trimers. Also, the differences between the oligomeric FCPs of *C. meneghiniana* and *P. tricornutum* with respect to their localization in a sucrose gradient remain enigmatic. An oligomeric FCP complex described as being hexa- to nonameric should be located very close to the PS fractions in the sucrose gradient, according to the present results from gelfiltration and the calculations of (32). However, it cannot be ruled out that the FCP complexes of *C. meneghiniana* and *P. tricornutum* behave differently when they are separated by SDC or gelfiltration. This might be due to a decreased stability of the oligomeric FCP of *C. meneghiniana* during separation either in a sucrose gradient or in a gelfiltration. The observed differences might also be caused by a different lipid composition of the oligomeric complexes of the two diatoms, which would lead to distinct surface mass/ratios and densities of the complexes, thus affecting their separation behavior in the SDC or gelfiltration. For *C. meneghiniana*, it was also shown that the oligomeric FCP complex exhibits a different polypeptide composition than the trimeric complex (18, 33). This is in contrast to our observation that both the oligomeric and the trimeric complexes have the same polypeptide composition and might additionally be responsible for the observed differences in the sucrose gradient and the gelfiltration.

It should also be noted that the FCPo complex of *P. tricornutum*, although it comigrates with the PS fractions both in the gelfiltration and the SDC separation, is not connected to the PS core complexes. If the FCPo would form a supercomplex with the PS core complex, as has been observed in higher plants (34, 35), this would lead to an extremely high molecular mass of the respective fraction. In the gelfiltration experiments, such a supercomplex would be characterized by a significantly shorter retention time compared with the PSII fractions isolated at higher detergent concentrations.

Another difference from the results obtained in refs 18 and 19 is our observation that under different solubilization conditions always one homogeneous FCP fraction was found.

This was especially obvious in the gelfiltration results and is significantly different from vascular plants, where besides the main LHCII trimer fraction, monomeric and dimeric LHC fractions could be separated (cf. Figure 2). In *P. tricornutum* monomeric, trimeric, and oligomeric antenna complexes do not seem to coexist, and the FCP complexes are either in a trimeric or higher oligomeric state. Monomeric FCP complexes could only be observed when the FCP or FCPo was subjected to freeze–thaw cycles or after a longer incubation of the fractions at room temperature (data not shown).

Under the mild solubilization conditions used in the present study, no other FCP fractions apart from the FCPo and FCP complexes were found. Especially, the FCP complex termed fraction D (19), which seems to be enriched in the XC pigments and exhibits a significantly lower molecular mass than the other FCP complexes, could not be observed. However, artificial disintegration of the FCP fraction by freezing followed by gelfiltration yielded, in addition to the monomeric FCPs, a further fraction with a retarded retention time, which was enriched in the XC pigments (data not shown). It may therefore be possible that the FCP complex termed fraction D represents an artifact of the respective solubilization and protein separation conditions.

With regard to the native state of the *P. tricornutum* antenna complex we propose, on the basis of the spectroscopic features (Figure 3), that the FCPo represents this state better than the trimeric FCP complex. It is important to note, however, that no clear spectral fingerprint was found for the FCPo compared to the FCP, which is again different from the results obtained by Büchel (18), where differences in the CD spectra between higher oligomers and trimers could be seen. This poses the possibility that the FCPo consists of two associated FCP trimers. The FCP trimer seems to be the stable basic unit of the *P. tricornutum* antenna system, which then assembles into antenna complexes of higher structural order. However, taking into account that DM/Chl ratios of 10 led to the occurrence of unstable oligomeric FCP complexes with molecular masses in between FCPo and FCP, we cannot rule out that the FCPo represents a hexameric unit composed of six monomers instead of two trimers.

The second important result of our present study is the assignment of the FCPs to the respective genes by MS/MS. To our knowledge, this is the first time that these pigment proteins in diatoms were identified on the protein level using MS. However, Rhiel and co-workers were already able to identify Fcp2, Fcp4, and Fcp6 using specific antibodies in *C. cryptica* (36–38). The analytical problem to identify each protein arises from the high sequence homologies of about 86–99% among the different *fcp* gene products (6). Thus, it is difficult to find all specific sequences to distinguish these six proteins in an in-gel digest. Moreover, the protein bands were not well separated because of the high sequence homologies and very similar molecular masses. Therefore, most peptides found in the digests allowed one to identify the protein group but not to distinguish among the isoforms. This was typically done by one or two tandem mass spectra or only the peptide masses. Therefore, it is not clear if the 19 kDa FCP band contains *fcpC*, *fcpD*, or both proteins, taking into account that they exhibit a sequence homology of 99% (6). Some weak signals, which were not accessible to tandem mass spectrometry, also indicated the presence of *fcpB* and *fcpE*. Although MALDI-MS is not a quantitative

technique, the high sequence homology of the peptides specific for either of the isoforms allows correlating the signal intensities to the quantities. In this respect, the dominant forms for the 19 kDa protein were *fcpC* and *fcpD* with a contamination of *fcpB*, and mostly *fcpE* for the 18 kDa band with minor quantities of *fcpA* and *fcpF*. Preliminary data from two-dimensional gel electrophoresis in combination with MS and MS/MS analyses indicate that the six *fcp* gene products cannot be clearly separated into single bands by SDS-PAGE alone, which was already implied by the pale smear between and above the two bands.

On the basis of HPLC pigment analyses and the concentration of PS and FCP fractions, our present study provides the information that the majority of the XC pigments are bound to the peripheral FCP antenna, which contains more than 95% of the total carotenoid. However, it also became obvious that the remaining carotenoid fraction that was found in the PS bands of the SDC was enriched in XC pigments (Figure 4C). This is in line with previous results (39). While in the FCP complexes the Fx/(Ddx + Dtx) ratio was around 6, it was approximately 1 in the PS bands. The enrichment of XC pigments in the PS fractions was accompanied by a significantly lower DES of the XC pigment pool as compared to the DES in the FCP fractions. The nature of the putative XC binding protein in the PS fractions, however, remains elusive. Possible candidates such as Fcp2 and Fcp4, which seem to be tightly associated with both photosystems in *C. cryptica* (38), were not detected in the present PS preparations. A 19.5 kDa protein, which was observed in the *P. tricornutum* PS fractions, did not yield reasonable sequence information and could therefore not be identified as an additional FCP. Taking into account that the assignment of the other FCPs to the family of fucoxanthin chlorophyll binding proteins by mass spectrometry was uncomplicated, the 19.5 kDa protein most likely does not belong to the classical FCPs. In a recent work, Fcp6/7 of *C. meneghiniana*, which is related to the LI818-protein of *C. reinhardtii* (40), was suggested to represent the XC-pigment binding protein of the diatom antenna (33). The whole genome data of *P. tricornutum* show that besides the classical FcpA-F, Lhcr-like FCPs, related to the red algal LHC, and LI818-like FCPs, related to the LI818s of *C. reinhardtii*, also exist (40–42). It might be possible that the 19.5 kDa protein associated with the *P. tricornutum* core complexes belongs to these protein families. Guglielmi et al. suggested that proteins in the range from 15–17 kDa represent the XC-binding proteins (19). In our preparations, the main protein band in this range was composed of the PsaD protein, which is involved in Fd-binding to PSI (43), and the PsaL protein. The function of the PsaL protein is still under debate, but taking into account that this protein in *A. thaliana* together with PsaH is suggested to bind photosynthetic pigments (44), it cannot be excluded that PsaL plays a role in Ddx binding. However, other weak protein bands observed in the 16–23 kDa range may belong to the LHC superfamily and are in addition likely candidates for XC pigment binding.

CONCLUSIONS

The presence of an oligomeric antenna in diatoms is in line with the oligomeric organization of the antenna complexes in different photoautotrophic groups. Purple photosynthetic bacteria possess oligomeric ring antenna structures

(45, 46). Cyanobacteria contain phycobilisomes that are large oligomeric complexes attached to the membrane (47). Green plants exhibit semicrystalline arrays of LHCII-PSII supercomplexes and large ordered macrodomains of LHCII (15–17). It was also shown for brown algae, organisms closely related to the diatoms, that they have an oligomeric FCP (48) that strongly resembles the FCPo described in this study. This type of organization is probably brought about by the high protein content of the thylakoid membrane and the high self-aggregation ability of the antenna complexes (49). Oligomeric antennas therefore seem to be the most widespread type of antenna organization for photoautotrophs.

ACKNOWLEDGMENT

We thank Mrs. Ilona Pfeiffer from the Microbiological Department of the University of Szeged for giving us the opportunity to use their French press.

REFERENCES

1. Archibald, J. M., and Keeling, P. J. (2002) Recycled plastids: a 'green movement' in eukaryotic evolution, *Trends Genet.* 18, 577–584.
2. Yoon, H. S., Hackett, J. D., Pinto, G., and Bhattacharya, D. (2002) The single, ancient origin of chromist plastids, *Proc. Natl. Acad. Sci. U.S.A.* 99, 15507–15512.
3. Pysznik, A. M., and Gibbs, S. P. (1992) Immunocytochemical localization of photosystem I and the fucoxanthin-chlorophyll-a/c light-harvesting complex in the diatom *Phaeodactylum tricornutum*, *Protoplasma* 166, 208–217.
4. Gibbs, S. P. (1962) The ultrastructure of the chloroplasts of algae, *J. Ultrastruct. Res.* 7, 418–435.
5. Anderson, J. M., and Aro, E. M. (1994) Grana stacking and protection of photosystem II in thylakoid membranes of higher plant leaves under sustained high irradiance - an hypothesis, *Photosynth. Res.* 41, 315–326.
6. Bhaya, D., and Grossman, A. R. (1993) Characterization of gene clusters encoding the fucoxanthin chlorophyll proteins of the diatom *Phaeodactylum tricornutum*, *Nucleic Acids Res.* 21, 4458–4466.
7. Eppard, M., and Rhiel, E. (1998) The genes encoding light-harvesting subunits of *Cyclotella cryptica* (Bacillariophyceae) constitute a complex and heterogeneous family, *Mol. Gen. Genomics* 260, 335–345.
8. Armbrust, E. V., Berges, J. A., Bowler, C., Green, B. R., Martinez, D., Putnam, N. H., Zhou, S. G., Allen, A. E., Apt, K. E., Bechner, M., Brzezinski, M. A., Chaal, B. K., Chiovitti, A., Davis, A. K., Demarest, M. S., Detter, J. C., Glavina, T., Goodstein, D., Hadi, M. Z., Hellsten, U., Hildebrand, M., Jenkins, B. D., Jurka, J., Kapitonov, V. V., Kroger, N., Lau, W. W. Y., Lane, T. W., Larimer, F. W., Lippmeier, J. C., Lucas, S., Medina, M., Montsant, A., Obornik, M., Parker, M. S., Palenik, B., Pazour, G. J., Richardson, P. M., Rynearson, T. A., Saito, M. A., Schwartz, D. C., Thamatrakoln, K., Valentin, K., Vardi, A., Wilkerson, F. P., and Rokhsar, D. S. (2004) The genome of the diatom *Thalassiosira pseudonana*: ecology, evolution, and metabolism, *Science* 306, 79–86.
9. Montsant, A., Jabbari, K., Maheswari, U., and Bowler, C. (2005) Comparative genomics of the pennate diatom *Phaeodactylum tricornutum*, *Plant Physiol.* 137, 500–513.
10. Friedman, A. L., and Alberty, R. S. (1986) Biogenesis and light regulation of the major light harvesting chlorophyll-protein of diatoms, *Plant Physiol.* 80, 43–51.
11. Fawley, M. W., and Grossman, A. R. (1986) Polypeptides of a light-harvesting complex of the diatom *Phaeodactylum tricornutum* are synthesized in the cytoplasm of the cell as precursors, *Plant Physiol.* 81, 149–155.
12. Caron, L., Remy, R., and Berkaloff, C. (1988) Polypeptide composition of light-harvesting complexes from some brown algae and diatoms, *FEBS Lett.* 229, 11–15.
13. Grossman, A. R., Manodori, A., and Snyder, D. (1990) Light-harvesting proteins of diatoms: Their relationship to the chlorophyll a/b binding proteins of higher plants and their mode of transport into plastids, *Mol. Gen. Genomics* 224, 91–100.

14. Durnford, D. G., Aebersold, R., and Green, B. R. (1996) The fucoxanthin-chlorophyll proteins from a chromophyte alga are part of a large multigene family: structural and evolutionary relationships to other light harvesting antennae, *Mol. Gen. Genomics* 253, 377–386.
15. Dekker, J. P., and Boekema, E. J. (2005) Supramolecular organization of thylakoid membrane proteins in green plants, *Biochim. Biophys. Acta* 1706, 12–39.
16. Garab, G., and Mustardy, L. (1999) Role of LHCII-containing macrodomains in the structure, function and dynamics of grana, *Aust. J. Plant Physiol.* 26, 649–658.
17. Boekema, E. J., van Breemen, J. F. L., van Roon, H., and Dekker, J. P. (2000) Arrangement of photosystem II supercomplexes in crystalline macrodomains within the thylakoid membrane of green plant chloroplasts, *J. Mol. Biol.* 301, 1123–1133.
18. Büchel, C. (2003) Fucoxanthin-chlorophyll proteins in diatoms: 18 and 19 kDa subunits assemble into different oligomeric states, *Biochemistry* 42, 13027–13034.
19. Guglielmi, G., Lavaud, J., Rousseau, B., Etienne, A. L., Houmard, J., and Ruban, A. V. (2005) The light-harvesting antenna of the diatom *Phaeodactylum tricornutum*: evidence for a diadinoxanthin-binding subcomplex, *FEBS J.* 272, 4339–4348.
20. Stransky, H., and Hager, A. (1970) Das Carotinoidmuster und die Verbreitung des lichtinduzierten Xanthophyllzyklus in verschiedenen Algenklassen V. Einzelne Vertreter der *Cryptophyceae*, *Euglenophyceae*, *Bacillariophyceae*, *Chrysophyceae* und *Phaeophyceae*, *Arch. Microbiol.* 73, 77–89.
21. Olaiola, M., LaRoche, J., Kolber, Z., and Falkowski, P. G. (1994) Non-photochemical fluorescence quenching and the diadinoxanthin cycle in a marine diatom, *Photosynth. Res.* 41, 357–370.
22. Arsalane, W., Rousseau, B., and Duval, J. C. (1994) Influence of the pool size of the xanthophyll cycle on the effects of light stress in a diatom: competition between photoprotection and photoinhibition, *Photochem. Photobiol.* 60, 237–243.
23. Lavaud, J., Rousseau, B., and Etienne, A. L. (2003) Enrichment of the light-harvesting complex in diadinoxanthin and implications for the nonphotochemical fluorescence quenching in diatoms, *Biochemistry* 42, 5802–5808.
24. Ruban, A. V., Lee, P. J., Wentworth, M., Young, A. J., and Horton, P. (1999) Determination of the stoichiometry and strength of binding of xanthophylls to the photosystem II light harvesting complexes, *J. Biol. Chem.* 274, 10458–10465.
25. Provasoli, L., McLaughlin, J. J. A., and Droop, M. R. (1957) The development of artificial media for marine algae, *Arch. Microbiol.* 25, 392–428.
26. Lohr, M., and Wilhelm, C. (2001) Xanthophyll synthesis in diatoms: quantification of putative intermediates and comparison of pigment conversion kinetics with rate constants derived from a model, *Planta* 212, 382–391.
27. Jensen, R. G., and Bassham, J. A. (1966) Photosynthesis by isolated chloroplasts, *Proc. Natl. Acad. Sci. U.S.A.* 56, 1095–1101.
28. Jeffrey, S. W., and Humphrey, G. F. (1975) New spectrophotometric equations for determining chlorophylls a, b, c1 and c2 in higher plants, algae and natural phytoplankton, *Biochem. Physiol. Pflanzen* 167, 191–194.
29. Kraay, G. W., Zapata, M., and Veldhuis, M. J. W. (1992) Separation of chlorophylls c1, c2, and c3 of marine phytoplankton by reversed-phase-C18-high-performance liquid chromatography, *J. Phycol.* 28, 708–712.
30. Wilhelm, C., Volkmar, P., Lohman, C., Becker, A., and Meyer, M. (1995) The HPLC-aided pigment analysis of phytoplankton cells as a powerful tool in water quality control, *Aqua (London)* 44, 132–141.
31. Laemmli, U. K. (1970) Cleavage of structural proteins during the assembly of the head of bacteriophage T4, *Nature* 227, 680–685.
32. Molik, S., Karnauchov, I., Weidlich, C. E., Herrmann, R. G., and Klossgen, R. B. (2001) The Rieske Fe/S protein of the cytochrome b(6)/f complex in chloroplasts: missing link in the evolution of protein transport pathways in chloroplasts? *J. Biol. Chem.* 276, 42761–42766.
33. Beer, A., Gundermann, K., Beckmann, J., and Buchel, C. (2006) Subunit composition and pigmentation of fucoxanthin-chlorophyll proteins in diatoms: evidence for a subunit involved in diadinoxanthin and diatoxanthin binding, *Biochemistry* 45, 13046–13053.
34. Boekema, E. J., Hankamer, B., Bald, D., Kruij, J., Nield, J., Boonstra, A. F., Barber, J., and Rogner, M. (1995) Supramolecular structure of the photosystem-II complex from green plants and cyanobacteria, *Proc. Natl. Acad. Sci. U.S.A.* 92, 175–179.
35. Boekema, E. J., van Roon, H., van Breemen, J. F. L., and Dekker, J. P. (1999) Supramolecular organization of photosystem II and its light-harvesting antenna in partially solubilized photosystem II membranes, *FEBS J.* 266, 444–452.
36. Westermann, M., and Rhiel, E. (2005) Localisation of fucoxanthin chlorophyll a/c-binding polypeptides of the centric diatom *Cyclotella cryptica* by immuno-electron microscopy, *Protoplasma* 225, 217–223.
37. Becker, F., and Rhiel, E. (2006) Immuno-electron microscopic quantification of the fucoxanthin chlorophyll a/c binding polypeptides Fcp2, Fcp4, and Fcp6 of *Cyclotella cryptica* grown under low- and high-light intensities, *Int. Microbiol.* 9, 29–36.
38. Brakemann, T., Schlormann, W., Marquardt, J., Nolte, M., and Rhiel, E. (2006) Association of fucoxanthin chlorophyll a/c-binding polypeptides with photosystems and phosphorylation in the centric diatom *Cyclotella cryptica*, *Protist* 157, 463–475.
39. Berkaloff, C., Caron, L., and Rousseau, B. (1990) Subunit organization of PSI particles from brown algae and diatoms: polypeptide and pigment analysis, *Photosynth. Res.* 23, 181–193.
40. Richard, C., Ouellet, H., and Guertin, M. (2000) Characterization of the LI818 polypeptide from the green unicellular alga *Chlamydomonas reinhardtii*, *Plant Mol. Biol.* 42, 303–316.
41. Eppard, M., Krumbein, W. E., von Haeseler, A., and Rhiel, E. (2000) Characterization of fcp4 and fcp12, two additional genes encoding light harvesting proteins of *Cyclotella cryptica* (Bacillariophyceae) and phylogenetic analysis of this complex gene family, *Plant Biology* 2, 283–289.
42. Green, B. R. (2003) The Evolution of Light-Harvesting Antennas, in *Light-Harvesting Antennas in Photosynthesis* (Green, B. R., and Parson, W. W., Eds.) pp 129–168, Kluwer Academic Publishers, Dordrecht, The Netherlands.
43. Setif, P., Fischer, N., Lagoutte, B., Bottin, H., and Rochaix, J. D. (2002) The ferredoxin docking site of photosystem I, *Biochim. Biophys. Acta* 1555, 204–209.
44. Ihalaenen, J. A., Jensen, P. E., Haldrup, A., van Stokkum, I. H. M., van Grondelle, R., Scheller, H. V., and Dekker, J. P. (2002) Pigment organization and energy transfer dynamics in isolated, photosystem I (PSI) complexes from *Arabidopsis thaliana* depleted of the PSI-G, PSI-K, PSI-L, or PSI-N subunit, *Biophys. J.* 83, 2190–2201.
45. Karrasch, S., Bullough, P. A., and Ghosh, R. (1995) The 8.5 Å projection map of the light-harvesting complex I from *Rhodospirillum rubrum* reveals a ring composed of 16 subunits, *EMBO J.* 14, 631–638.
46. Bahatyrova, S., Frese, R. N., Siebert, C. A., Olsen, J. D., van der Werf, K. O., van Grondelle, R., Niederman, R. A., Bullough, P. A., Otto, C., and Hunter, C. N. (2004) The native architecture of a photosynthetic membrane, *Nature* 430, 1058–1062.
47. MacColl, R. (1998) Cyanobacterial phycobilisomes, *J. Struct. Biol.* 124, 311–334.
48. Katoh, T., Mimuro, M., and Takaichi, S. (1989) Light-harvesting particles isolated from a brown alga, *Dictyota dichotoma*. A supramolecular assembly of fucoxanthin-chlorophyll-protein complexes, *Biochim. Biophys. Acta* 976, 233–240.
49. Garab, G., Lohner, K., Laggner, P., and Farkas, T. (2000) Self-regulation of the lipid content of membranes by non-bilayer lipids: a hypothesis, *Trends Plant Sci.* 5, 489–494.

BI7008344